


Long-time persistence of hydrodynamic memory boosts microparticle transport

Sean L. Seyler 

Department of Physics, Arizona State University, Tempe, Arizona 85287, USA

Steve Pressé *

Department of Physics and School of Molecular Sciences, Arizona State University, Tempe, Arizona 85287, USA



(Received 15 June 2019; published 7 October 2019)

In a viscous fluid, the past motion of an accelerating particle is retained as an imprint on the vorticity field, which decays slowly as $t^{-3/2}$. At low Reynolds number, the Basset-Boussinesq-Oseen (BBO) equation correctly describes nonuniform particle motion, capturing hydrodynamic memory effects associated with this slow algebraic decay. Using the BBO equation, we numerically simulate driven single-particle transport to show that memory effects persist indefinitely under rather general driving conditions. In particular, when driving forces do not vary smoothly, hydrodynamic memory substantially lowers the effective transport friction. Remarkably, this enables coasting over a spatially uneven potential that otherwise traps particles modeled with pure Stokes drag. Our results provide direct physical insight into the role of particle-fluid coupling in nonequilibrium microparticle transport.

DOI: [10.1103/PhysRevResearch.1.032003](https://doi.org/10.1103/PhysRevResearch.1.032003)

Introduction. In the pioneering work of Alder and Wainwright [1], molecular dynamics simulations of hard-spheres liquid argon revealed a long-time tail in the velocity auto-correlation function, which decays as $t^{-3/2}$. Whereas standard Langevin theory predicts exponential decay over a Brownian relaxation time τ_B , this algebraic decay is caused by viscous coupling between nonuniform particle motion and unsteady flow generated in the ambient fluid [1–3]. As a particle accelerates, so does the fluid it displaces, inducing a virtual mass force that augments the particle’s apparent inertia. The particle also imparts momentum to the fluid as vorticity, which diffuses over a particle radius in a kinematic time τ_v proportional to the fluid density. A particle that translates over its own radius before the ambient fluid relaxes thus experiences a delayed self-interaction due to the vorticity generated by its past motion [4]. This retarded force is known as the Basset history force, which underlies the slow $t^{-3/2}$ decay associated with hydrodynamic memory.

These unsteady forces, which arise when $\tau_v \simeq \tau_B$ where the (fluid) bath’s inertia becomes significant, are captured by the Basset-Boussinesq-Oseen (BBO) equation [5–7] [Eq. (1)], a remarkably general description that applies not just to macroscopic objects; it applies to Brownian motion well into the nanoscale [8–10], as substantiated by recent experiments directly probing the microscopic velocities and colored noise spectra of optically trapped particles [11–16]. Theoretical efforts have been essential to understanding the BBO

description [17], not to mention yielding analytical solutions for simple external forces that furnish physical intuition at the level of individual trajectories. Although analytical solutions are infeasible for general forcing, advances in the computation of the history force have made numerical simulation increasingly viable [18–20].

These important advances notwithstanding, it is common to neglect fluid inertia *a priori*—often at low Reynolds number—especially because memoryless models are ubiquitous, conceptually simple, and computationally efficient. It may be reasoned, perhaps, that memory effects can be safely ignored if both τ_v and τ_B are much shorter than relevant observation timescales, such as the time to establish steady state behavior. The memoryless assumption, however, tacitly implies that $\tau_v \ll \tau_B$; these timescales are not well separated in dense media (e.g., liquids), even when $\text{Re} \ll 1$ [21–23]. This is indeed the case for the myriad mesoscopic phenomena at submicron scales such as conformational changes in biomacromolecules [24,25], unsteady motion of microswimmers [26–28], active subcellular transport [29–31], and colloidal flows [4,32], not to mention particle dispersion in turbulent flows and the atmosphere [33–37], sediment transport in rivers and pipes [38–42], and other engineering applications [43–46].

In this Rapid Communication, we unambiguously show that neglecting the history force can lead to qualitatively incorrect particle transport under general forcing conditions, including oscillating steady states. Building upon previous analytical results, we use numerical simulations to demonstrate that hydrodynamic memory does not merely protract the transient relaxation to steady state but also persists *indefinitely* under a significant parameter regime, implying that the BBO description may be necessary regardless of observation timescales. We begin by examining time-dependent square-wave driving to physically illustrate how the history force,

*spresse@asu.edu

which models the transient retention of momentum by the fluid bath, improves the conversion efficiency of input work into kinetic energy of a particle. For driving frequencies below τ_v^{-1} , hydrodynamic memory considerably lowers the effective friction, which, as we show, leads to enhanced transport in a tilted periodic potential, whereas pure Stokes dissipation tends to suppress itinerant behavior.

Problem overview. Consider a microsphere [47] of radius R , mass m , and density ρ_s in an incompressible fluid of density ρ and viscosity η , with no-slip boundary conditions. In the limit of low Reynolds number and Mach number, nonuniform motion is described by the BBO equation [5–7],

$$m_e \dot{\mathbf{v}} + \zeta_s \mathbf{v}(t) + \zeta_s \sqrt{\frac{\tau_v}{\pi}} \int_{t_0}^t \frac{\dot{\mathbf{v}}(\tau)}{\sqrt{t-\tau}} d\tau = \mathbf{F}(\mathbf{x}, t). \quad (1)$$

The second term—the quasisteady component—is the familiar Stokes drag with friction coefficient $\zeta_s = 6\pi\eta R$, which defines the Brownian relaxation time, $\tau_B = m_e/\zeta_s$. Unsteady flow introduces two additional forces: (1) the virtual mass force, where $m_a = \frac{2}{3}\pi R^3 \rho$ is the added mass and $m_e = m + m_a$ is the *effective mass*; (2) the Basset history force, a convolution over past acceleration. Here, the kinematic time, $\tau_v = R^2/\nu$, which depends on the kinematic viscosity of the fluid, $\nu = \eta/\rho$, quantifies the time for vorticity to diffuse over a distance R .

It is instructive to consider Eq. (1) in dimensionless form. First, we introduce the following dimensional scales, which we use in the ensuing analyses (also cf. Arminski and Weinbaum [48]):

$$t_c = \tau_B, \quad \mathcal{E}_c = k_B T, \quad v_c = v_{\text{th}}, \quad (2)$$

where $v_{\text{th}} = \sqrt{k_B T/m_e}$ is the thermal speed, and the dimensionless time is $\tilde{t} = t/t_c$, dimensionless velocity is $\tilde{v} = v/v_c$, and so on. Accordingly, length is scaled by $L_c = v_{\text{th}}\tau_B$, mass by $M_c = m_e$, force by $F_c = k_B T/v_{\text{th}}\tau_B$, power by $P_c = k_B T/\tau_B$, and friction by ζ_s . By introducing $\beta = \frac{9\rho}{2\rho_s + \rho}$, one may show that the particle and fluid timescales are related by $\beta = \tau_v/\tau_B$ [48,49]. Redefining \tilde{t} as t , \tilde{v} as v , and so on, one obtains the following dimensionless form:

$$\dot{\mathbf{v}} + \mathbf{v}(t) + \sqrt{\frac{\beta}{\pi}} \int_{t_0}^t \frac{\dot{\mathbf{v}}(\tau)}{\sqrt{t-\tau}} d\tau = \mathbf{F}(\mathbf{x}, t). \quad (3)$$

In the present analyses, we assume neutral buoyancy—pertinent to many processes in liquid water—so $\rho_s = \rho$, $\beta = 3$, and the history term is of order unity by Eq. (3). In this case, the history force can be neglected only if \mathbf{F} varies in such a way that a particle always moves near terminal speed (i.e., $\dot{\mathbf{v}} \sim 0$).

Many strategies have been used to either derive Eq. (1) itself (or closely related forms) or shed light on the algebraic decay of the correlation functions, including techniques based on Navier-Stokes [3,50,51], fluctuating hydrodynamics [52–54] (i.e., Landau-Lifschitz Navier-Stokes [2]), mode coupling theory [55–57], and kinetic theory [58,59], among others [1,60,61]. In the case of hydrodynamic Brownian motion, \mathbf{F} may consist of deterministic time-dependent and conservative components, as well as thermal fluctuations [49,62,63]; respectively, $\mathbf{F}(x, t) = \mathbf{f}(t) - \nabla U(\mathbf{x}) + \boldsymbol{\xi}(t)$. By the second fluctuation-dissipation theorem (FDT), the Basset memory

kernel implies that $\boldsymbol{\xi}$ is a colored noise process [64,65]. In the limit of vanishing fluid inertia, $\rho_s \gg \rho$, $\tau_v \ll \tau_B$, and the history force vanishes; $\boldsymbol{\xi}$ then becomes a white noise process and Eq. (1) reduces to a memoryless Markovian description (i.e., a conventional Langevin equation).

The full non-Markovian dynamics of Eq. (1) are quite complicated, which obfuscates the physical picture. We therefore focus on zero-temperature dynamics in one dimension; the finite-temperature case will be treated in a follow-up study. We obtain numerical solutions using an extended phase space method wherein an exponential sum approximates the memory kernel [66]. A distinct advantage of this approach—sometimes called *Markovian embedding*—is that it also systematically generates the correct thermal noise correlations (obeying the FDT) as a weighted sum of white noises [67–70]. While the numerical method is not the focus of this study, our results support the practicability of such an approach in modeling driven hydrodynamic Brownian motion [69]. For brevity, we refer to spherical particles obeying Eq. (1) as *BBO beads*; likewise, we have *Stokes beads* when fluid inertia is neglected (i.e., $\beta \rightarrow 0$ and $m_e \rightarrow m$).

Energy flow for a square pulse. The case of a finite-duration square or sawtooth pulse acting on a particle—with and without the Basset history force—was studied analytically by Arminski and Weinbaum [48]. It was shown that the maximum bead displacement Δx_{max} depends only on the total impulse $J_{\text{max}} = \int F dt$ and not the dynamics or wave form; in dimensionless form, $\Delta x_{\text{max}} = J_{\text{max}}$, an important result we use later. Thus, assuming beads start and end at rest, the history term only acts to alter the details of bead motion on intermediate timescales. Here, we revisit the square pulse case to: (1) examine the history force from the standpoint of energy flow; (2) establish a point of contact between our numerical results and known analytical solutions. Accordingly, we consider BBO and Stokes beads, initially at rest, acted upon by a force $f(t) = f_0$ for $0 \leq t \leq \tau_0$. We then compute the net work and instantaneous power term-by-term for the equation of motion and directly compare BBO and Stokes beads. It is seen that the history force transiently retains energy, which can be redistributed to a BBO bead as kinetic energy (i.e., momentum) at later times.

Figure 1 shows results for a “long” pulse (relative to τ_B) of duration $\tau_0 = 10\tau_B$, where $f_0 = \frac{1}{10}F_c$ and $\Delta x_{\text{max}} = L_c$. Due to the history force and, to a lesser extent, the virtual mass force, a BBO bead responds more gradually than a Stokes bead [Fig. 1(b)], taking tens of τ_B to reach 80% of its long-time displacement [Fig. 1(a)]. On the other hand, since the force is constant during the driving phase ($t < \tau_B$), the total input work and peak power is evidently lower for a BBO bead [Figs. 1(c) and 1(d)]. Figure 1(b) details how input work is apportioned between the instantaneous kinetic energy, total heat loss (through Stokes dissipation), and fluid stress energy lost through vorticity diffusion (through the history term).

In particular, Stokes dissipation irreversibly converts kinetic energy into heat and is always positive. By contrast, the instantaneous power dissipation through the history force abruptly switches sign shortly into the relaxation phase [$t > 10\tau_B$; Fig. 1(d)], illustrating the transfer of energy back to the BBO bead from the fluid. This particular effect is less pronounced for short- and medium-duration pulses, though

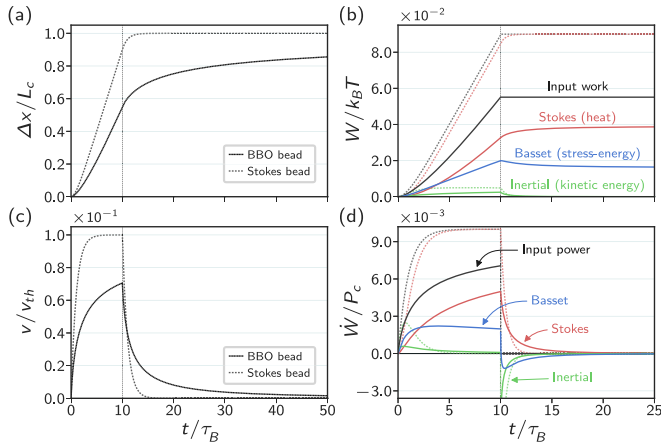


FIG. 1. Stokes versus BBO beads for a single square pulse. BBO beads have a smoother net displacement (a) and instantaneous velocity (c) due to the history force, which returns energy to the bead for $t > 10\tau_B$ [(b), (d); blue]. Stokes beads dissipate energy purely as heat [(b), (d); dashed red]. Pulse duration $\tau_0 = 10\tau_B$ and amplitude $f_0 = \frac{1}{10}F_c$. All panels: Stokes, dotted lines; BBO, solid lines. Panels (a), (c): Shared horizontal axes. Panels (b), (d): Shared horizontal axes; lines color coded by (force) term.

the overall intermediate-time behavior is quite similar [71]. In any case, a BBO bead takes longer to displace than a Stokes bead but, since hydrodynamic memory improves momentum retention, the same displacement is achieved with less work.

Temporal square wave forcing. Extending the single-pulse results to a square wave is straightforward if the pulses are spaced arbitrarily far apart; since each pulse is isolated, it is clear that the energy saved per pulse (due to the history force) can be sustained over an arbitrary number of cycles. Likewise, it is reasonable to expect that the energy saved per pulse will remain finite as long as the pulse spacing is nonzero, leading to an efficiency enhancement in the transport of a BBO bead. To this end, we quantify the trade-off between input energy, total displacement, and overall transport speed by defining an effective friction ζ_t , by analogy with Stokes' law,

$$\bar{F}_t = \zeta_t \bar{v}_t, \quad (4)$$

where we have introduced the *effective velocity*,

$$\bar{v}_t = \frac{1}{t} \int_0^t v(\tau) d\tau = \frac{\Delta x_t}{t}, \quad (5)$$

and the *effective driving force*,

$$\bar{F}_t = \frac{1}{\Delta x_t} \int_0^t F(x, \tau) v(\tau) d\tau = \frac{W_t}{\Delta x_t}, \quad (6)$$

where W_t is the net input work and $\Delta x_t = x(t) - x(0)$ is net displacement. Note that force balance in steady state implicitly defines an effective drag force via $\bar{F}_t \sim -\bar{F}_{\text{drag}}$. Using Eqs. (4) to (6), it is easy to compute running estimates of the effective friction.

We now consider BBO and Stokes beads driven by square waves with period $\tau = 10\tau_B$, pulse width τ_0 , and amplitude f_0 , holding fixed the impulse per cycle, $J_{\text{cyc}} = f_0\tau_0 = \sqrt{m_e k_B T}$. Figure 2 compares the effective displacement, velocity, driving force, and friction as pulse width is varied. By $t = 250\tau_B$,

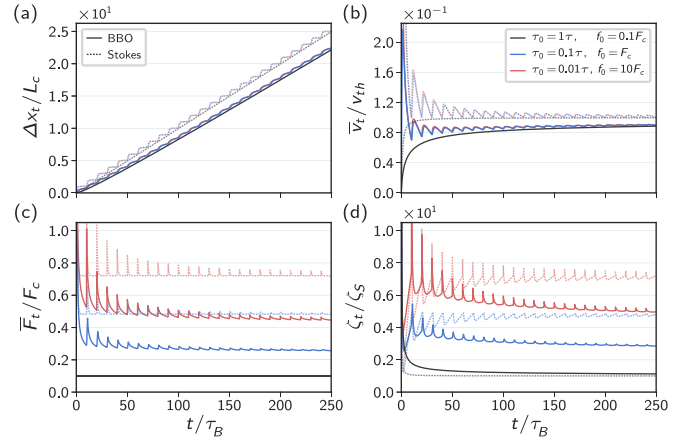


FIG. 2. For time-periodic driving with fixed impulse per cycle, BBO (solid lines) and Stokes (dotted) beads achieve comparable net displacements (a) and effective velocities (b), but BBO beads are more easily driven (c), reducing effective friction (d). Period $\tau = 10\tau_B$; pulse width τ_0 and force f_0 are varied.

BBO and Stokes beads achieve around 90% and 100%, respectively, of the maximum possible displacement ($\Delta x_{\text{max}} = 25L_c$) [Fig. 2(a)], consistent with the expectation that the total impulse determines the long-time displacement. Moreover, as J_{cyc} also determines the cycle-averaged momentum input rate, BBO and Stokes beads achieve similar effective velocities [Fig. 2(b)] [72].

For always-on forcing (i.e., 100% duty cycle), the effective driving (and drag) force is fixed and the effective friction quickly approaches ζ_s [black; Figs. 2(c) and 2(d)], which is the expected quasisteady behavior. By contrast, increasing the abruptness of the pulses (shorter duration, larger magnitude) increases the effective driving force, especially in the case of Stokes beads [red and blue, Fig. 2(c)]. Given that the history force attenuates acceleration during the forcing phase [cf. Fig. 1(c)], which reduces the velocity and, in turn, input work [cf. Fig. 1(b)], this is expected. It follows that a BBO bead's effective friction is comparable to a Stokes bead's for a constant (always-on) force but is lower for intermittent forcing.

Tilted periodic potential with gaps. We now consider beads in a tilted “periodic gap potential,” which dovetails with the preceding square-wave analysis. The potential has a wavelength λ , overall tilt F_0 , and a piecewise-linear construction that alternates between downward-sloped segments of constant, positive force and *gaps*, flat segments of length d with zero force (Fig. 3, black or gray line). This simple construction is sufficient to illustrate the role of the Basset term in the (un)trapping of beads while providing a clear physical picture. We also show that our conclusions extend straightforwardly to experimentally realizable models such as the tilted washboard potential, which has broad physical relevance [73–78].

Beads are initialized with zero velocity at the top of a downhill segment so that they initially feel a constant force of magnitude $F_{\text{max}} = F_0(\frac{\lambda}{\lambda-d})$ [79]. Upon reaching the first gap, the total energy input is $W = -\Delta U_0$, where $\Delta U_0 = -F_0\lambda$, and coasting begins. It is clear that a bead must coast past the first gap so as to achieve sustained transport; otherwise, it

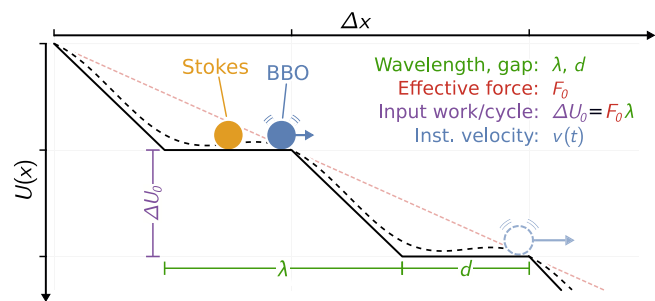


FIG. 3. Tilted periodic gap potential (black line) with wavelength λ , gaps of length d , and tilt F_0 (red dashes). Here, an itinerant BBO bead progresses beyond the first gap, but a Stokes bead is trapped. Downhill regions have a slope $F_{\max} = F_0(\frac{\lambda}{\lambda-d})$, which steepens as the gap size d increases. A tilted washboard potential (dashed black line) with local minima is shown for comparison.

becomes trapped indefinitely. Recalling that $\Delta x_{\max} = J_{\max}$, it can be seen that knowing the gap size d and initial momentum input is sufficient to determine whether trapping occurs. The momentum input is just the initial impulse, $J^* = F_{\max} t^*$, where t^* is the time to arrive at the first gap; since F_{\max} is constant, t^* controls whether trapping occurs, though it is determined by solving the specific equation of motion. However, $t_{\text{BBO}}^* \geq t_{\text{Stokes}}^*$ because the history force reduces the acceleration of a BBO bead [Fig. 2(b)], so we can deduce that $J_{\text{BBO}}^* \geq J_{\text{Stokes}}^*$. Since long-time displacement only depends on J^* , BBO beads coast farther than Stokes beads; if BBO beads get trapped, so do Stokes beads.

For a bead that becomes itinerant, the average energy input per unit distance is simply given by the tilt F_0 , which also sets a lower bound on the effective driving or drag force, $\bar{F}_t \geq F_0$. Once a bead covers a distance large compared to the wavelength ($\Delta x_t/\lambda \gg 1$), then $W \propto \Delta x_t$ and Eq. (6) implies that $\bar{F}_t \rightarrow F_0$. Recall that time-periodic driving, by contrast, fixes the momentum input rate, which largely constrains the effective velocity but *not* the effective driving force [cf. Figs. 2(b) and 2(c)]. Accordingly, we expect that the effective velocity will be the prevailing factor that determines the effective friction ζ_t in a tilted periodic potential.

Figure 4 depicts a representative comparison between BBO and Stokes beads for a large gap ($d = \frac{1}{2}\lambda$), small gap ($d = \frac{1}{4}\lambda$), and no gap ($d = 0$), holding wavelength ($\lambda = L_c$) and tilt ($F_0 = \frac{1}{5}F_c$) fixed. Whereas all BBO beads are able to escape, Stokes beads are trapped by the first gap, both large and small [Fig. 4(a)]. Small gaps have a slight effect on a BBO bead's velocity, while large gaps noticeably impede motion, at least initially [Fig. 4(b)]. Note that itinerant beads—all BBO beads and the Stokes bead when there is no gap—have effective driving forces \bar{F}_t that do indeed approach $\frac{1}{5}F_c$ at long times [Fig. 4(c)]; the final value of \bar{F}_t for trapped beads is set by the final displacement after coming to rest [red and blue dashed lines, Fig. 4(c)]. While the effective friction ζ_t measurably decreases over several hundred τ_B for the BBO beads, ζ_t diverges for the trapped Stokes beads since their effective velocities drop to zero [Fig. 4(d)].

The results for a comparable tilted washboard potential are also consistent with expectations [80]. Moreover, extending

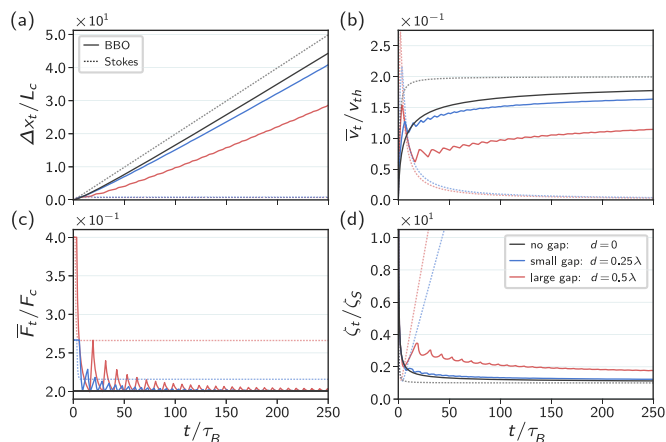


FIG. 4. In a tilted potential, BBO beads (solid lines) can traverse gaps that trap Stokes beads (dotted). Net displacement (a) and effective velocity (b) determine, respectively, net energy and average power input. The effective driving force (c) is constrained by the tilt F_0 , so the effective friction (d) is dictated by the effective velocity. Wavelength $\lambda = L_c$ and tilt $F_0 = \frac{1}{5}F_c$, so $\Delta U_0 = \frac{1}{5}k_B T$. Initial slope $F_{\max} = \frac{F_c}{5}(\frac{\lambda}{\lambda-d})$.

the analysis of the tilted gap potential over a wider parameter space that spans different combinations of wavelength λ , tilt F_0 , and gap size d confirms that a Stokes bead is always trapped when a BBO bead is trapped [81]. Impeding the motion of Stokes beads—through gaps or local minima and barriers—markedly increases the effective friction; the effect on BBO beads is comparatively minor and, moreover, diminishes in time. What is perhaps more striking is that even the relatively smooth landscape of a critically tilted washboard (where no trapping is possible) has a rather large effect on a Stokes bead, more than doubling the effective friction in comparison to a constant force.

Discussion. Overall, a Stokes bead in transport appears to be remarkably sensitive to variations in the external driving force. When fluid inertia is taken into account, however, the Basset history force moderates momentum and energy flow between bead and environment, smoothing the bead's response [Figs. 2(a) and 2(b)]. From a physical standpoint, a BBO bead extends “into the bath” in the sense that the ambient fluid can temporarily retain a portion of the total momentum and energy, a consequence being that a BBO bead can, in effect, transiently store and access “latent kinetic energy.” This aspect of the history force is prominent when the external force drops precipitously, as exemplified by the “long” square pulse case [Fig. 1(c)]. In general, any input work that accelerates a bead beyond its (cycle-averaged) effective velocity will be wasted as heat over the latter part of a cycle [after $F(t)$ falls below the average \bar{F}]. However, the history force redistributes some of the surplus work at later times as kinetic energy; the remaining fluid momentum will be gradually lost to vorticity diffusion, and yet it is decidedly less efficient if all available momentum is carried entirely by a (Stokes) bead itself—this increases (Stokes) dissipation [Fig. 1(d)], which grows quadratically with the momentum.

That a Stokes bead dissipates excess (kinetic) energy more quickly than a BBO bead reflects a key difference in the

physical models: as a driving force becomes intermittent, or a potential landscape rough, the effective friction increases; but, if fluid inertia were erroneously neglected, a (Stokes) bead would be driven unnaturally quickly toward a quasisteady state [consistent with the value of $F(t)$], exacerbating the apparent increase in the effective friction and hindering transport. While pure Stokes dissipation (too) hastily sheds surplus energy from a fluctuating energy source, the history force assists a (BBO) bead in utilizing the available energy more effectively, thereby enhancing transport efficiency. Indeed, this effect does not depend so much on forcing frequency itself as it does on the time rate of change of the driving force \dot{F} , which, when nonzero, drives a particle away from quasisteady motion. It is also interesting to note that as long as the driving force has a period larger than roughly τ_v , there is a transitory period of momentum accumulation in the fluid as it is continually agitated by a driven bead [82]. This is evident from the continual decline of the effective friction over hundreds of τ_b for both time-periodic driving [red, Fig. 2(d)] and the tilted periodic potentials [red, Fig. 4(d) and Fig. 6(d) in the Supplemental Material].

The aim of this Rapid Communication has been to elucidate the physical mechanism underlying hydrodynamic memory, examine the impact of the Basset history force on deterministic microparticle transport, and build a foundation for investigating hydrodynamic Brownian motion at finite temperature, where hydrodynamic memory drives the long-time persistence of thermal fluctuations [11–15]. In the case of purely time-dependent external forcing, thermal averages should agree with the deterministic results. For periodic tilted potentials like the tilted washboard, we anticipate qualitative agreement with the present results, namely that an ensemble of BBO beads may be able to attain a larger effective velocity than a Stokes bead ensemble when initialized on a downhill region (i.e., where the initial force is positive). In particular, hydrodynamic memory hedges against uncertainty in

fluctuating sources of energy, including both thermal and external forces. Less trivially, however, we also anticipate dynamical bistability, where individual beads may assume either trapped (or *locked*) or itinerant (or *running*) states, undergoing intermittent transitions between them. In particular, the interplay between a periodic driving force and transition rates can give rise to resonance phenomena, such as stochastic resonance [83], which are sensitive to correlations in the noise [84,85] as well as the damping terms [86]. These questions, however, have yet to be explored in the context of the physically relevant case of hydrodynamic Brownian motion as described by Eq. (1).

Other avenues of exploration include the generalization and connection to the compressible flow case [8,32,87–89]. In view of Ref. [9], where it was shown that even tagged fluid particles closely follow BBO dynamics, the present results are also germane to temperature and pressure control algorithms in molecular dynamics simulations, especially as extended phase space approaches show promise in improving the kinetic consistency of thermostats [90,91], as well as deriving dynamically consistent and computationally viable coarse-graining schemes for complex atomistic systems [92–95]. Indeed, such approaches can be brought to bear on the question of stochastic transport efficiency of Brownian motors [96], including linear molecular motors like kinesin [97–99]; viscoelastic properties of the fluid environment (e.g., the cytosolic medium) can also be modeled within the extended phase space framework [70,100–102].

Acknowledgments. The authors are indebted to Julian Lee, Charles Seyler, Michael Howard, Kyle Seyler, Ian Kenney, Zeliha Kilic, Ian Welland, and David Ferry for fruitful discussions and critical feedback on the manuscript. This work was supported by ARO Grant No. W911NF-17-1-0162 on “Multi-Dimensional and Dissipative Dynamical Systems: Maximum Entropy as a Principle for Modeling Dynamics and Emergent Phenomena in Complex Systems.”

-
- [1] B. J. Alder and T. E. Wainwright, Decay of the velocity autocorrelation function, *Phys. Rev. A* **1**, 18 (1970).
- [2] L. D. Landau and E. M. Lifschitz, *Fluid Mechanics*, 3rd ed. (Pergamon Press, Oxford, 1966), Vol. 6.
- [3] R. Zwanzig and M. Bixon, Hydrodynamic theory of the velocity correlation function, *Phys. Rev. A* **2**, 2005 (1970).
- [4] J. T. Padding and A. A. Louis, Hydrodynamic interactions and Brownian forces in colloidal suspensions: Coarse-graining over time and length scales, *Phys. Rev. E* **74**, 031402 (2006).
- [5] J. Boussinesq, Sur la résistance qu’oppose un liquide indéfini en repos, sans pesanteur, au mouvement varié d’une sphère solide qu’il mouille sur toute sa surface, quand les vitesses restent bien continues et assez faibles pour que leurs carrés et produits soient négligeables, *C. R. Acad. Sci. Paris*. **100**, 935 (1885).
- [6] A. B. Basset, III. On the motion of a sphere in a viscous liquid, *Philos. Trans. R. Soc. London A* **179**, 43 (1888).
- [7] C. W. Oseen, *Neuere Methoden und Ergebnisse in der Hydrodynamik* (Akademische Verlagsgesellschaft, Leipzig, 1927).
- [8] D. Lesnicki, R. Vuilleumier, A. Carof, and B. Rotenberg, Molecular Hydrodynamics from Memory Kernels, *Phys. Rev. Lett.* **116**, 147804 (2016).
- [9] D. Lesnicki and R. Vuilleumier, Microscopic flow around a diffusing particle, *J. Chem. Phys.* **147**, 094502 (2017).
- [10] K. Mizuta, Y. Ishii, K. Kim, and N. Matubayasi, Bridging the gap between molecular dynamics and hydrodynamics in nanoscale Brownian motions, *Soft Matter* **15**, 4380 (2019).
- [11] T. Li, S. Kheifets, D. Medellin, and M. G. Raizen, Measurement of the instantaneous velocity of a Brownian particle, *Science* **328**, 1673 (2010).
- [12] R. Huang, I. Chavez, K. M. Taute, B. Lukić, S. Jeney, M. G. Raizen, and E.-L. Florin, Direct observation of the full transition from ballistic to diffusive Brownian motion in a liquid, *Nat. Phys.* **7**, 576 (2011).
- [13] T. Franosch, M. Grimm, M. Belushkin, F. M. Mor, G. Foffi, L. Forró, and S. Jeney, Resonances arising from hydrodynamic memory in Brownian motion, *Nature (London)* **478**, 85 (2011).

- [14] A. Jannasch, M. Mahamdeh, and E. Schäffer, Inertial Effects of a Small Brownian Particle Cause a Colored Power Spectral Density of Thermal Noise, *Phys. Rev. Lett.* **107**, 228301 (2011).
- [15] S. Kheifets, A. Simha, K. Melin, T. Li, and M. G. Raizen, Observation of Brownian motion in liquids at short times: Instantaneous velocity and memory loss, *Science* **343**, 1493 (2014).
- [16] J. Mo and M. G. Raizen, Highly resolved brownian motion in space and in time, *Annu. Rev. Fluid Mech.* **51**, 403 (2019).
- [17] See, for instance, [48,103–107], and, more recently, [108–111]; for techniques for transforming the BBO equation, see [112–117]; for a contemporary perspective on the problem of Brownian motion, see [118] and references therein.
- [18] M. A. T. van Hinsberg, J. H. M. ten Thije Boonkamp, and H. J. H. Clercx, An efficient, second order method for the approximation of the Basset history force, *J. Comput. Phys.* **230**, 1465 (2011).
- [19] A. Daitche, Advection of inertial particles in the presence of the history force: Higher order numerical schemes, *J. Comput. Phys.* **254**, 93 (2013).
- [20] P. A. Moreno-Casas and F. A. Bombardelli, Computation of the Basset force: Recent advances and environmental flow applications, *Environ. Fluid Mech.* **16**, 193 (2016).
- [21] H. A. Lorentz, L. Silberstein, and A. P. H. Trivelli, *Lectures on Theoretical Physics* (Macmillan and Company, Ltd., London, 1927), Vol. 1.
- [22] R. M. Mazo, *Brownian Motion: Fluctuations, Dynamics, and Applications* (Oxford University Press, Oxford, 2008).
- [23] S. Kim and S. J. Karrila, *Microhydrodynamics: Principles and Selected Applications* (Butterworth-Heinemann, Boston, 1991).
- [24] D. A. Beard and T. Schlick, Inertial stochastic dynamics. I. Long-time-step methods for Langevin dynamics, *J. Chem. Phys.* **112**, 7313 (2000).
- [25] D. A. Beard and T. Schlick, Inertial stochastic dynamics. II. Influence of inertia on slow kinetic processes of supercoiled DNA, *J. Chem. Phys.* **112**, 7323 (2000).
- [26] J. R. Howse, R. A. L. Jones, A. J. Ryan, T. Gough, R. Vafabakhsh, and R. Golestanian, Self-Motile Colloidal Particles: From Directed Propulsion to Random Walk, *Phys. Rev. Lett.* **99**, 048102 (2007).
- [27] S. Wang and A. M. Ardekani, Unsteady swimming of small organisms, *J. Fluid Mech.* **702**, 286 (2012).
- [28] H. Jashnsaz, M. Al Juboori, C. Weistuch, N. Miller, T. Nguyen, V. Meyerhoff, B. McCoy, S. Perkins, R. Wallgren, B. D. Ray, K. Tsekouras, G. G. Anderson, and S. Pressé, Hydrodynamic hunters, *Biophys. J.* **112**, 1282 (2017).
- [29] D. Houtman, I. Pagonabarraga, C. P. Lowe, A. Esseling-Ozdoba, A. M. C. Emons, and E. Eiser, Hydrodynamic flow caused by active transport along cytoskeletal elements, *Europhys. Lett.* **78**, 18001 (2007).
- [30] C. P. Brangwynne, G. H. Koenderink, F. C. MacKintosh, and D. A. Weitz, Cytoplasmic diffusion: Molecular motors mix it up, *J. Cell Biol.* **183**, 583 (2008).
- [31] R. Kapral and A. S. Mikhailov, Stirring a fluid at low Reynolds numbers: Hydrodynamic collective effects of active proteins in biological cells, *Phys. D (Amsterdam)* **318-319**, 100 (2016).
- [32] G. Jung and F. Schmid, Frequency-dependent hydrodynamic interaction between two solid spheres, *Phys. Fluids* **29**, 126101 (2017).
- [33] M. W. Reeks, The transport of discrete particles in inhomogeneous turbulence, *J. Aerosol Sci.* **14**, 729 (1983).
- [34] R. Mei, R. J. Adrian, and T. J. Hanratty, Particle dispersion in isotropic turbulence under Stokes drag and Basset force with gravitational settling, *J. Fluid Mech.* **225**, 481 (1991).
- [35] S. Yang and L. G. Leal, A note on memory-integral contributions to the force on an accelerating spherical drop at low Reynolds number, *Phys. Fluids A* **3**, 1822 (1991).
- [36] L. M. Sosnoskie, T. M. Webster, D. Dales, G. C. Rains, T. L. Grey, and A. S. Culpepper, Pollen grain size, density, and settling velocity for Palmer amaranth (*Amaranthus palmeri*), *Weed Sci.* **57**, 404 (2009).
- [37] M. A. T. van Hinsberg, H. J. H. Clercx, and F. Toschi, Enhanced settling of nonheavy inertial particles in homogeneous isotropic turbulence: The role of the pressure gradient and the Basset history force, *Phys. Rev. E* **95**, 023106 (2017).
- [38] W. H. Graf, *Hydraulics of Sediment Transport* (Water Resources Publication, New York, 1984).
- [39] J. S. Bridge and S. J. Bennett, A model for the entrainment and transport of sediment grains of mixed sizes, shapes, and densities, *Water Resour. Res.* **28**, 337 (1992).
- [40] T. Hvitved-Jacobsen, J. Vollertsen, and N. Tanaka, Wastewater quality changes during transport in sewers: An integrated aerobic and anaerobic model concept for carbon and sulfur microbial transformations, *Water Sci. Technol.* **38**, 257 (1998).
- [41] Cao Zhixian, Equilibrium near-bed concentration of suspended sediment, *J. Hydraul. Eng.* **125**, 1270 (1999).
- [42] J. W. Delleur, New results and research needs on sediment movement in urban drainage, *J. Water Resour. Plan. Manag.* **127**, 186 (2001).
- [43] E. E. Michaelides, Review: The transient equation of motion for particles, bubbles, and droplets, *J. Fluids Eng.* **119**, 233 (1997).
- [44] E. E. Michaelides, *Particles, Bubbles and Drops: Their Motion, Heat and Mass Transfer* (World Scientific Publishing, Singapore, 2006).
- [45] M. Jalaal, D. D. Ganji, and G. Ahmadi, Analytical investigation on acceleration motion of a vertically falling spherical particle in incompressible Newtonian media, *Adv. Powder Technol.* **21**, 298 (2010).
- [46] Z. Yin, Z. Wang, B. Liang, and L. Zhang, Initial velocity effect on acceleration fall of a spherical particle through still fluid, *Math. Probl. Eng.* **2017**, 9795286 (2017).
- [47] M. Vert, Y. Doi, K.-H. Hellwich, M. Hess, P. Hodge, P. Kubisa, M. Rinaudo, and F. Schué, Terminology for biorelated polymers and applications (IUPAC Recommendations 2012), *Pure Appl. Chem.* **84**, 377 (2012).
- [48] L. Arminski and S. Weinbaum, Effect of waveform and duration of impulse on the solution to the Basset-Langevin equation, *Phys. Fluids* **22**, 404 (1979).
- [49] F. Mainardi, in *Fractals and Fractional Calculus in Continuum Mechanics*, edited by A. Carpinteri and F. Mainardi (Springer, Vienna, 1997), Vol. 378, p. 291.
- [50] C. M. Tchen, Mean value and correlation problems connected with the motion of small particles suspended in a turbulent fluid, Ph.D. thesis, Delft University of Technology, 1947.

- [51] M. R. Maxey and J. J. Riley, Equation of motion for a small rigid sphere in a nonuniform flow, *Phys. Fluids* **26**, 883 (1983).
- [52] T. S. Chow and J. J. Hermans, Effect of inertia on the Brownian motion of rigid particles in a viscous fluid, *J. Chem. Phys.* **56**, 3150 (1972).
- [53] E. H. Hauge and A. Martin-Löf, Fluctuating hydrodynamics and Brownian motion, *J. Stat. Phys.* **7**, 259 (1973).
- [54] D. Bedeaux and P. Mazur, Brownian motion and fluctuating hydrodynamics, *Physica (Amsterdam)* **76**, 247 (1974).
- [55] M. H. Ernst, E. H. Hauge, and J. M. J. van Leeuwen, Asymptotic Time Behavior of Correlation Functions, *Phys. Rev. Lett.* **25**, 1254 (1970).
- [56] M. H. Ernst, E. H. Hauge, and J. M. J. van Leeuwen, Asymptotic time behavior of correlation functions and mode-mode coupling theory, *Phys. Lett. A* **34**, 419 (1971).
- [57] M. H. Ernst, E. H. Hauge, and J. M. J. van Leeuwen, Asymptotic time behavior of correlation functions. I. Kinetic terms, *Phys. Rev. A* **4**, 2055 (1971).
- [58] J. R. Dorfman and E. G. D. Cohen, Velocity Correlation Functions in Two and Three Dimensions, *Phys. Rev. Lett.* **25**, 1257 (1970).
- [59] Y. Pomeau and P. Résibois, Time dependent correlation functions and mode-mode coupling theories, *Phys. Rep.* **19**, 63 (1975).
- [60] A. Widom, Velocity fluctuations of a hard-core Brownian particle, *Phys. Rev. A* **3**, 1394 (1971).
- [61] H. T. Davis and G. Subramanian, Velocity fluctuations of a Brownian particle: Widom's model, *J. Chem. Phys.* **58**, 5167 (1973).
- [62] E. Fodor, D. S. Grebenkov, P. Visco, and F. van Wijland, Generalized Langevin equation with hydrodynamic backflow: Equilibrium properties, *Phys. A (Amsterdam)* **422**, 107 (2015).
- [63] J. Tóthová and V. Lisý, A note on the fluctuation–dissipation relation for the generalized Langevin equation with hydrodynamic backflow, *Phys. Lett. A* **380**, 2561 (2016).
- [64] H. Mori, Transport, collective motion, and Brownian motion, *Prog. Theor. Phys.* **33**, 423 (1965).
- [65] R. Kubo, The fluctuation-dissipation theorem, *Rep. Prog. Phys.* **29**, 255 (1966).
- [66] See Supplemental Material at <http://link.aps.org/supplemental/10.1103/PhysRevResearch.1.032003> for details of the numerical method.
- [67] R. Kupferman, Fractional kinetics in Kac-Zwanzig heat bath models, *J. Stat. Phys.* **114**, 291 (2004).
- [68] M. Ferrario and P. Grigolini, The non-Markovian relaxation process as a “contraction” of a multidimensional one of Markovian type, *J. Math. Phys.* **20**, 2567 (1979).
- [69] P. Siegle, I. Goychuk, and P. Hänggi, Markovian embedding of fractional superdiffusion, *Europhys. Lett.* **93**, 20002 (2011).
- [70] A. D. Baczewski and S. D. Bond, Numerical integration of the extended variable generalized Langevin equation with a positive Prony representable memory kernel, *J. Chem. Phys.* **139**, 044107 (2013).
- [71] See Supplemental Material at <http://link.aps.org/supplemental/10.1103/PhysRevResearch.1.032003>, Figs. 1 and 2, for the results for “short” and “medium” pulses.
- [72] In the long-time limit under a *constant* external force, the quasisteady approximation is valid (and the Basset force vanishes); physically, this means the effective velocity of BBO and Stokes beads will converge to the same terminal velocity, which corresponds to the problem of a particle falling through a (less-dense) viscous fluid under the force of gravity [103–105,107].
- [73] A. Ajdari and J. Prost, Free-flow electrophoresis with trapping by a transverse inhomogeneous field, *Proc. Natl. Acad. Sci. USA* **88**, 4468 (1991).
- [74] D. Reguera, J. M. Rubi, and A. Perez-Madrid, Controlling anomalous stresses in soft field-responsive systems, *Phys. Rev. E* **62**, 5313 (2000).
- [75] G. Grüner, A. Zawadowski, and P. M. Chaikin, Nonlinear Conductivity and Noise due to Charge-Density-Wave Depinning in NbSe₃, *Phys. Rev. Lett.* **46**, 511 (1981).
- [76] Y. Yu and S. Han, Resonant Escape over an Oscillating Barrier in Underdamped Josephson Tunnel Junctions, *Phys. Rev. Lett.* **91**, 127003 (2003).
- [77] W. T. Coffey, Y. P. Kalmykov, S. V. Titov, L. Cleary, and W. J. Dowling, Master equation in phase space applied to the quantum Brownian motion in a tilted periodic potential, *J. Phys. A: Math. Theor.* **45**, 105002 (2012).
- [78] See for instance [69,86,119–127] for theoretical and numerical investigations, as well as [128,129] and references therein; for experimental realizations of the tilted washboard potential, see [130–136].
- [79] We verified that starting beads with a finite initial velocity does not change our conclusions.
- [80] See Supplemental Material at <http://link.aps.org/supplemental/10.1103/PhysRevResearch.1.032003>, Fig. 6, for Stokes versus BBO comparison in the tilted washboard potential.
- [81] See Supplemental Material at <http://link.aps.org/supplemental/10.1103/PhysRevResearch.1.032003>, Figs. 7 and 8, for tilted potential results with different parameter combinations.
- [82] See Supplemental Material at <http://link.aps.org/supplemental/10.1103/PhysRevResearch.1.032003>, Figs. 3–5, exploring different forcing frequencies.
- [83] B. McNamara and K. Wiesenfeld, Theory of stochastic resonance, *Phys. Rev. A* **39**, 4854 (1989).
- [84] Z.-W. Bai and P. Wang, Escape rate of Brownian particles from a metastable potential well under time derivative Ornstein-Uhlenbeck noise, *Eur. Phys. J. B* **89**, 75 (2016).
- [85] Y. Jin, W. Xie, and K. Liu, Noise-induced resonances in a periodic potential driven by correlated noises, *Proc. IUTAM* **22**, 267 (2017).
- [86] S. Saikia, The role of damping on stochastic resonance in a periodic potential, *Phys. A (Amsterdam)* **416**, 411 (2014).
- [87] R. Zwanzig and M. Bixon, Compressibility effects in the hydrodynamic theory of Brownian motion, *J. Fluid Mech.* **69**, 21 (1975).
- [88] H. Metiu, D. W. Oxtoby, and K. F. Freed, Hydrodynamic theory for vibrational relaxation in liquids, *Phys. Rev. A* **15**, 361 (1977).
- [89] M. Parmar, A. Haselbacher, and S. Balachandar, Generalized Basset-Boussinesq-Oseen Equation for Unsteady Forces on a Sphere in a Compressible Flow, *Phys. Rev. Lett.* **106**, 084501 (2011).
- [90] J. E. Basconi and M. R. Shirts, Effects of temperature control algorithms on transport properties and kinetics in molecular dynamics simulations, *J. Chem. Theory Comput.* **9**, 2887 (2013).

- [91] H. Ness, L. Stella, C. D. Lorenz, and L. Kantorovich, Applications of the generalized Langevin equation: Towards a realistic description of the baths, *Phys. Rev. B* **91**, 014301 (2015).
- [92] C. Hijón, P. Español, E. Vanden-Eijnden, and R. Delgado-Buscalioni, Mori-Zwanzig formalism as a practical computational tool, *Faraday Discuss.* **144**, 301 (2009).
- [93] Z. Li, X. Bian, X. Li, and G. E. Karniadakis, Incorporation of memory effects in coarse-grained modeling via the Mori-Zwanzig formalism, *J. Chem. Phys.* **143**, 243128 (2015).
- [94] Z. Li, H. S. Lee, E. Darve, and G. E. Karniadakis, Computing the non-Markovian coarse-grained interactions derived from the Mori-Zwanzig formalism in molecular systems: Application to polymer melts, *J. Chem. Phys.* **146**, 014104 (2017).
- [95] Y. Yoshimoto, Z. Li, I. Kinefuchi, and G. E. Karniadakis, Construction of non-Markovian coarse-grained models employing the Mori-Zwanzig formalism and iterative Boltzmann inversion, *J. Chem. Phys.* **147**, 244110 (2017).
- [96] L.-R. Nie and D.-C. Mei, Effect of correlated noises on Brownian motor, *Phys. Lett. A* **373**, 3816 (2009).
- [97] W. Hwang and C. Hyeon, Quantifying the heat dissipation from a molecular motor's transport properties in nonequilibrium steady states, *J. Phys. Chem. Lett.* **8**, 250 (2017).
- [98] T. Ariga, M. Tomishige, and D. Mizuno, Nonequilibrium Energetics of Molecular Motor Kinesin, *Phys. Rev. Lett.* **121**, 218101 (2018).
- [99] W. Hwang and C. Hyeon, Energetic costs, precision, and transport efficiency of molecular motors, *J. Phys. Chem. Lett.* **9**, 513 (2018).
- [100] I. Goychuk, Viscoelastic subdiffusion: From anomalous to normal, *Phys. Rev. E* **80**, 046125 (2009).
- [101] P. Siegle, I. Goychuk, P. Talkner, and P. Hänggi, Markovian embedding of non-Markovian superdiffusion, *Phys. Rev. E* **81**, 011136 (2010).
- [102] I. Goychuk, Viscoelastic subdiffusion in a random Gaussian environment, *Phys. Chem. Chem. Phys.* **20**, 24140 (2018).
- [103] H. Villat, *Leçons sur les Fluides Visqueux* (Gauthier-Villars, Paris, 1943), pp. 84–112.
- [104] L. M. Brush, H.-W. Ho, and B.-C. Yen, Accelerated motion of a sphere in a viscous fluid, *J. Hydraul. Div.* **90**, 149 (1964).
- [105] F. Sy, J. W. Taunton, and E. N. Lightfoot, Transient creeping flow around spheres, *AIChE J.* **16**, 386 (1970).
- [106] E. J. Hinch, Application of the Langevin equation to fluid suspensions, *J. Fluid Mech.* **72**, 499 (1975).
- [107] C.-S. Yih, *Fluid Mechanics*, corrected ed. (West River Press, Ann Arbor, MI, 1977).
- [108] C. F. M. Coimbra and R. H. Rangel, General solution of the particle momentum equation in unsteady Stokes flows, *J. Fluid Mech.* **370**, 53 (1998).
- [109] A. Venkatalaxmi, B. S. Padmavathi, and T. Amaranath, A general solution of unsteady Stokes equations, *Fluid Dyn. Res.* **35**, 229 (2004).
- [110] B. U. Felderhof, Effect of the wall on the velocity autocorrelation function and long-time tail of Brownian motion, *J. Phys. Chem. B* **109**, 21406 (2005).
- [111] S. Ganga Prasath, V. Vasani, and R. Govindarajan, Accurate solution method for the Maxey-Riley equation, and the effects of Basset history, *J. Fluid Mech.* **868**, 428 (2019).
- [112] E. E. Michaelides, A novel way of computing the Basset term in unsteady multiphase flow computations, *Phys. Fluids A* **4**, 1579 (1992).
- [113] A. Belmonte, J. T. Jacobsen, and A. Jayaraman, Monotone solutions of a nonautonomous differential equation for a sedimenting sphere, *Electron. J. Diff. Eq.* **2001**, 1 (2001).
- [114] M. H. Kobayashi and C. F. M. Coimbra, On the stability of the Maxey-Riley equation in nonuniform linear flows, *Phys. Fluids* **17**, 113301 (2005).
- [115] Y. D. Sobral, T. F. Oliveira, and F. R. Cunha, On the unsteady forces during the motion of a sedimenting particle, *Powder Technol.* **178**, 129 (2007).
- [116] Y. V. Visitskii, A. G. Petrov, and M. M. Shunderyuk, The motion of a particle in a viscous fluid under gravity, vibration and Basset's force, *J. Appl. Math. Mech.* **73**, 548 (2009).
- [117] I. S. Vodop'yanov, A. G. Petrov, and M. M. Shunderyuk, Unsteady sedimentation of a spherical solid particle in a viscous fluid, *Fluid Dyn.* **45**, 254 (2010).
- [118] X. Bian, C. Kim, and G. E. Karniadakis, 111 years of Brownian motion, *Soft Matter* **12**, 6331 (2016).
- [119] M. Bandyopadhyay, S. Dattagupta, and M. Sanyal, Diffusion enhancement in a periodic potential under high-frequency space-dependent forcing, *Phys. Rev. E* **73**, 051108 (2006).
- [120] A. I. Shushin, Diffusion in a tilted periodic potential: Specific properties of motion in the underdamped limit, *Chem. Phys.* **370**, 244 (2010).
- [121] I. G. Marchenko, I. I. Marchenko, and V. I. Tkachenko, Temperature-abnormal diffusivity in underdamped spatially periodic systems, *JETP Lett.* **106**, 242 (2017).
- [122] T. Guérin and D. S. Dean, Universal time-dependent dispersion properties for diffusion in a one-dimensional critically tilted potential, *Phys. Rev. E* **95**, 012109 (2017).
- [123] G. Costantini and F. Marchesoni, Threshold diffusion in a tilted washboard potential, *Europhys. Lett.* **48**, 491 (1999).
- [124] P. Siegle, I. Goychuk, and P. Hänggi, Origin of Hyperdiffusion in Generalized Brownian Motion, *Phys. Rev. Lett.* **105**, 100602 (2010).
- [125] W. L. Reenbohn and M. C. Mahato, Relative stability of dynamical states and stochastic resonance in a sinusoidal potential, *Phys. Rev. E* **88**, 032143 (2013).
- [126] B. Lindner and I. M. Sokolov, Giant diffusion of underdamped particles in a biased periodic potential, *Phys. Rev. E* **93**, 042106 (2016).
- [127] J.-M. Zhang and J.-D. Bao, Transition of multidiffusive states in a biased periodic potential, *Phys. Rev. E* **95**, 032107 (2017).
- [128] H. D. Vollmer and H. Risken, Eigenvalues and their connection to transition rates for the Brownian motion in an inclined cosine potential, *Z. Phys. B* **52**, 259 (1983).
- [129] P. Jung and H. Risken, Eigenvalues for the extremely underdamped Brownian motion in an inclined periodic potential, *Z. Phys. B* **54**, 357 (1984).
- [130] J. E. Curtis and D. G. Grier, Structure of Optical Vortices, *Phys. Rev. Lett.* **90**, 133901 (2003).
- [131] C.-S. Guo, X. Liu, J.-L. He, and H.-T. Wang, Optimal annulus structures of optical vortices, *Opt. Express* **12**, 4625 (2004).
- [132] S.-H. Lee and D. Grier, Robustness of holographic optical traps against phase scaling errors, *Opt. Express* **13**, 7458 (2005).

- [133] S.-H. Lee and D. G. Grier, Giant Colloidal Diffusivity on Corrugated Optical Vortices, *Phys. Rev. Lett.* **96**, 190601 (2006).
- [134] M. Evstigneev, O. Zvyagolskaya, S. Bleil, R. Eichhorn, C. Bechinger, and P. Reimann, Diffusion of colloidal particles in a tilted periodic potential: Theory versus experiment, *Phys. Rev. E* **77**, 041107 (2008).
- [135] M. Siler and P. Zemánek, Particle jumps between optical traps in a one-dimensional (1D) optical lattice, *New J. Phys.* **12**, 083001 (2010).
- [136] M. P. N. Juniper, R. Besseling, D. G. A. L. Aarts, and R. P. A. Dullens, Acousto-optically generated potential energy landscapes: Potential mapping using colloids under flow, *Opt. Express* **20**, 28707 (2012).